Thermoelectric properties in $Ca_3Co_{4-x}Mn_xO_y$ ceramics

G. Constantinescu[1], M. A. Torres[1], Sh. Rasekh[1], P. Bosque[2], M. A. Madre[1], J. C. Diez[1], A. Sotelo[1]

[1]ICMA (Universidad de Zaragoza-CSIC), C/María de Luna 3, E-50018, Zaragoza (Spain)

[2]Centro Universitario de la Defensa de Zaragoza. Academia General Militar. Ctra. de Huesca s/n. 50090-Zaragoza (Spain).

Abstract

$Ca_3Co_{4-x}Mn_xO_y$ polycrystalline thermoelectric ceramics with small amounts of Mn have been prepared by the classical solid state method. XRD data have shown that $Ca_3Co_4O_9$ is the major phase, with small amounts of the $Ca_3Co_2O_6$ one. Moreover, they show that the Mn has been incorporated into these two phases. Electrical resistivity decreases, compared with the values for undoped samples, with Mn content until a minimum for the 0.03-doped ones, increasing for higher Mn substitution. Seebeck coefficient does not change in all the measured temperature range, independently of Mn content. The improvement in electrical resistivity leads about 30 % higher power factor values for the 0.03 Mn-doped samples than the obtained in the undoped ones. The maximum power factor at 800 ºC, around 0.28 mW K^{-2} m^{-1} is close to the obtained in much higher density samples, clearly indicating the good thermoelectric properties of these samples.

Keywords: Ceramics; Cobaltites; Electrical properties; Thermopower.

Corresponding author: A. Sotelo

e-mail: asotelo@unizar.es

Address: ICMA (CSIC-Universidad de Zaragoza) C/Mª de Luna, 3; 50018-Zaragoza; Spain

Tel: +34 976762617

Fax: +34 976761957

Introduction

Thermoelectric (TE) materials are gaining interest due to their intrinsic properties, as they can directly transform a temperature difference to electrical power. The conversion efficiency of such materials is usually quantified by the figure of merit ($ZT=T\ S^2\ \rho^{-1}\ \kappa^{-1}$), where S is Seebeck coefficient, ρ electrical resistivity, κ thermal conductivity, and T is the absolute temperature.[1] In this expression, the electrical part ($S^2\ \rho^{-1}$), called power factor (PF) is often used to characterise its performances. These materials have focused attention for their use in practical applications as waste heat recovery devices[2] or solar thermoelectric generators,[3] which can help to reduce fuel consumption raising the efficiency of classical energy transformation systems.[2]

Some practical applications of TE devices, built with intermetallic materials, can be found, as energy harvesting in vehicles exhaust. However, due to their degradation and/or oxidation under air at high temperatures, they cannot be applied in devices working at these high temperatures. Moreover, they are usually composed of heavy and toxic elements, as Te, Sb, etc., which are not environmentally friendly. The limitations due to the nature of these intermetallic materials were surpassed by the discovery of high thermoelectric performances in $Na_2Co_2O_4$ ceramics[4] which are characterized by the absence of heavy elements and their higher chemical stability at high temperatures. Since then, many works have been made on the cobalt-based ceramics for high temperature applications, mainly on the $Ca_3Co_4O_9$,[5,6] $Bi_2Sr_2Co_2O_x$,[7,8] $Bi_2Ca_2Co_2O_x$,[9,10] and $Bi_2Ba_2Co_2O_x$[11,12] systems with high thermoelectric properties and working temperatures.

Crystallographic studies of CoO-based thermoelectric ceramics have shown that these materials can be described by a monoclinic structure which is, in turn, composed of two different layers. These layers are alternatively stacked and consist of a common conductive CdI_2-type hexagonal CoO_2 layer with a two-dimensional triangular lattice and a block layer composed of insulating rock-salt-type (RS) layers. The two sublattices (RS block and CdI_2-type CoO_2 layer) possess common a- and c-axis lattice parameters and β angles, but different b-axis length, causing a misfit along the b-direction.[13] The high structural anisotropy of these materials leads to the formation of plate-like grains during the crystallisation process which can be exploited to preferentially align the grains using different processes. As a consequence, they produce the alignment of the conducting planes leading to a raise on the electrical properties of the bulk material. Numerous methods have been reported to be efficient to produce well aligned grains, in these or in similar anisotropic systems, such as hot uniaxial pressing,[14] spark plasma sintering,[15] laser floating zone melting (LFZ),[16] electrically assisted laser floating zone (EALFZ),[17] *etc*. On the other hand, the main drawbacks of these methods are due to different factors, as the relatively long treatments, the high costs associated with the processes and/or the strong dependence on the growth or the texturing speed.[14,15,18,19]

It has also been reported that the Seebeck coefficient and electrical resistivity values are governed by the incommensurability ratio and/or the charge of the RS block layer between the CoO_2 ones[20] which provides the basis for the modification of thermoelectric properties by cation substitutions. The most common ones are based on the substitution of an alkaline-earth,[21,22] Co,[23,24] or

Bi[25,26] which have demonstrated their suitability for improving the materials performances.

The aim of this work is studying the effect of small substitutions of Co by Mn on the microstructure and high temperature thermoelectric properties of $Ca_3Co_{4-x}Mn_xO_y$ when it is prepared using the classical solid state synthesis route.

Experimental

$Ca_3Co_{4-x}Mn_xO_y$ polycrystalline ceramic materials, with x = 0.00, 0.01, 0.03, and 0.05, were prepared by the conventional solid state route using commercial $CaCO_3$ (Panreac, 98 + %), Co_2O_3 (Aldrich, 98 + %), and Mn_2O_3 (Aldrich, 99 %) powders as starting materials. They were weighed in the appropriate proportions, mixed and ball milled for 30 minutes at 300 rpm, in acetone media, in an agate ball mill. The slurry has been heated under infrared radiation until all the acetone has been evaporated. The dry mixture was then manually milled and thermally treated twice at 750 and 800 ºC for 12h under air, with an intermediate manual grinding to assure the total decomposition of $CaCO_3$. After thermal treatment, the powders were uniaxially pressed at 400 MPa for 1 minute in order to obtain green ceramic parallelepipeds (approximately 3 mm x 3 mm x 14 mm) and sintered at 910 ºC for 24 h with a final furnace cooling. Powder X-ray diffraction (XRD) patterns have been recorded in order to identify the different phases in the thermoelectric sintered materials. Data have been collected at room temperature, with 2θ ranging between 5 and 60 degrees, using a Rigaku D/max-B X-ray powder diffractometer working with Cu Kα radiation using a graphite monochromator.

Microstructural observations were performed on longitudinal sections and fractured surfaced of the samples, using a Field Emission Scanning Electron Microscope (FESEM, Carl Zeiss Merlin) fitted with an energy dispersive X-ray spectrometer (EDX). Micrographs of the samples surfaces have been used to analyze the different phases and their distribution. Apparent density measurements have been performed on several samples for each composition after sintering, using 4.677 g cm^{-3} as theoretical density.[27]

Oxygen content has been determined by cerimetric titration following the procedure described in previous works.[6] Electrical resistivity and Seebeck coefficient were simultaneously determined by the standard dc four-probe technique in a LSR-3 measurement system (Linseis GmbH), in the steady state mode and at temperatures ranging from 50 to 800 ºC under He atmosphere. From the resistivity values, the activation energy and the relative carrier concentration for each sample have been estimated. Moreover, with the electrical resistivity and thermopower data, the power factor has been calculated in order to determine the samples performances. These properties have been compared with the results obtained in the undoped samples and with those reported in the literature at low temperatures (~ 50 ºC), where oxygen diffusion is negligible, to avoid the influence of the atmosphere on the compared values.

Results and discussion

Powder XRD patterns for the different $Ca_3Co_{4-x}Mn_xO_y$ samples are displayed in Fig. 1 (from 5 to 40º for clarity). From these data, it is clear that all the samples are mainly composed by the thermoelectric $Ca_3Co_4O_9$ phase. As can be seen in

Fig. 1a, corresponding to the undoped samples, the highest peaks have been associated to the thermoelectric $Ca_3Co_4O_9$ phase, indicated by the reflection planes, in agreement with previously reported data,[28] where a monoclinic unit cell (#12, C12/m1) has been used. On the other hand, the peak at around 28.65 degrees (indicated by • in Fig. 1d) corresponds to the (111) diffraction plane of Si used as reference. Moreover, the peaks identified by * in Fig. 1 have been associated to the $Ca_3Co_2O_6$ phase, in agreement with previously reported data,[29] with a rhombohedral unit cell (#167, $R\bar{3}cH$). From these data, it seems that no significant difference on the amount of both phases can be found. The main differences between the XRD patterns is due to the preferential orientation of the grains, as can be deduced from the variation observed in the relative intensities of (00l) planes belonging to the $Ca_3Co_4O_9$ phase, with respect to the other ones. This effect can be associated to the samples preparation which can induce different preferential grain orientations in the powders. Furthermore, Mn doping does not appreciably change the phases proportions. On the other hand, no Mn based secondary phase has been detected with this technique, which is a clear indication that Mn has been incorporated in the $Ca_3Co_4O_9$ and/or $Ca_3Co_2O_6$ structures. Moreover, no changes on the peaks angles or on the FWHM have been detected, probably due to the similar sizes of Co and Mn. General SEM observations performed on representative fractured sections of the samples are shown in Fig. 2. In the micrographs, it can be clearly seen that both samples possess very similar microstructure, indicating that Mn doping does not modify it, in the small amounts used in this work. Other feature observed in these micrographs is the porosity, observed as black contrast in the figure, which seems to be very similar in all cases. In order to confirm this

observation, apparent density measurements have been performed for all samples. At least three samples for each composition were measured for three times to minimize measurement errors. The obtained results showed that all samples possess very similar densities which are about 71 % of the theoretical one in all cases, confirming the SEM observations. These relatively low densities can be easily explained due to the fact that the sintering temperature (910 ºC) is far from the melting temperature of this system (~ 1350 ºC), leading to a very slow densification kinetics.[30]

When observing the samples surfaces, they show roughly the same microstructures, described by the representative micrograph, performed on the 0.03 Mn doped samples, displayed in Fig. 3. In the micrograph, two different phases can be observed, the grey plate-like grains (identified by EDX as $Ca_3Co_4O_9$), and a very similar contrast grains with different shape (indicated by #1 in the picture) corresponding to the $Ca_3Co_2O_6$ secondary phase. EDX analysis of the different phases has shown that Mn substitutes Co in the $Ca_3Co_4O_9$ phase in small proportions (from less than 0.01 in the 0.01 Mn doped samples, to a maximum of about 0.02 for the 0.05 Mn doped ones), while higher Mn content has been found in the $Ca_3Co_2O_6$ phase reaching, in some grains, to substitute about one half of the Co in this phase.

Fig. 4 shows the variation of the Seebeck coefficient with the temperature, as a function of the Mn doping. In the plot, it can be clearly seen that the sign of the thermopower is positive for the entire measured temperature range, which confirms a conduction mechanism mainly governed by holes. The values of the Seebeck coefficient increase with the temperature, with very similar values and behaviour for all the samples. The obtained values at room temperature (~ 135

$\mu V\ K^{-1}$) are slightly higher than those reported elsewhere (~ 125 $\mu V\ K^{-1}$) at the same temperature.[31] On the other hand, the maximum Seebeck coefficient value (~ 215 $\mu V\ K^{-1}$) obtained in this work at 800 ºC is significantly higher than the values obtained for $Ca_3Co_4O_9$ samples prepared by autocombustion method and consolidated by spark plasma sintering (150 and 165 $\mu V\ K^{-1}$ measured parallel and perpendicular to the applied load, respectively) at the same temperature.[32] Moreover, it is also higher than the obtained in $Ca_2Co_2O_5$ ceramics prepared by a homogeneous precipitation route (around 175 $\mu V\ K^{-1}$).[33] The similar values obtained for all samples indicate that small Mn addition does not affect, in a great extent, the $Ca_3Co_4O_9$ conduction band.[34]

The absolute oxygen content was determined on sintered samples by cerimetric analysis. For each sample four determinations were performed, showing a reproducibility of around $\pm$ 0.008 for each sample. The obtained mean values are approximately the same and correspond to mean Co valences of ~ 3.15. These results agree with the measured room temperature Seebeck values which are roughly the same for all the samples.

The temperature dependence of electrical resistivity, as a function of the Mn content, is shown in Fig. 5. The ρ (T) curves show a decrease of resistivity when Mn is added, compared with the undoped samples. All the curves show a semiconducting-like ($d\rho/dT < 0$) behaviour, from room temperature to around 400 ºC, in agreement with previously reported data in this system where the charge transport process is a hole hopping from Co^{4+} to Co^{3+}.[35] At higher temperatures, this behaviour changes to a metallic-like ($d\rho/dT > 0$) one where the charge carriers are transported in the valence or conduction band.[24] In these doped samples, room temperature resistivity values decrease for the 0.01

and 0.03 Mn doped samples, and then increase for the 0.05 Mn content. The decrease of room temperature resistivity values with Mn addition is in agreement with previous works which demonstrate that the raise in the rock-salt layer dimensions (due to the higher ionic radii of Mn^{2+}, compared with the Co^{2+} one) produce a decrease of resistivity.[21] The raise of resistivity for Mn contents higher than 0.03 is related with the increase on the crystal defects which decrease the carriers mobility. The lowest measured room temperature resistivity values (~ 16 mΩ cm for the 0.03 Mn-substituted samples) are close to the values obtained for $Ca_3Co_4O_9$ samples produced by spark plasma sintering (~ 13 mΩ cm).[15] Moreover, the values at around 800 ºC (about 17 mΩ cm for the 0.03 Mn-substituted samples) is much lower than the measured in $Ca_2Co_2O_5$ samples prepared by homogeneous coprecipitation (~ 41 mΩ cm).[33] Taking into account the lower density values obtained in samples prepared by the solid state method, compared with the measured in spark plasma sintering prepared ones, the measured resistivity in the Mn doped samples is much lower than the expected in low density samples.

In order to evaluate the thermoelectric performances of these materials, the power factor has been calculated using the electrical resistivity and Seebeck coefficient data and plotted as a function of temperature in Fig. 6. When considering PF values at about 50 ºC (~ room temperature), it can be clearly seen that the Mn-doped samples possess higher PF values than the undoped ones (between 10 to 30 %). The highest PF value obtained at 800 ºC (around 0.28 mW K^{-2} m^{-1}) for the 0.03 Mn-doped samples is ~ 30 % higher than the obtained for the undoped samples. This maximum PF value is much higher than the obtained in solid state sintered nanopowders with Mn content of 0.3 (0.124

mW K^{-2} m^{-1}),[36] and is around the obtained in samples with 0.2 Mn substitution prepared by sol-gel and sintered using the spark plasma sintering technique (about 0.27 mW K^{-2} m^{-1}).[37] Moreover, it is also close to the obtained in samples prepared by high pressure technique (~ 0.33 mW K^{-2} m^{-1}).[31] In any case, the values obtained in this work are more impressive if it is taken into account that the values reported in the literature have been obtained in samples prepared by more sophisticated methods which produce higher density materials.

All these data indicate that small Mn additions can improve significantly the thermoelectric performances, in terms of PF, of $Ca_3Co_4O_9$ ceramics, thus approaching them to their commercial and practical applications.

Conclusions

This paper demonstrates that small Mn substitutions for Co in $Ca_3Co_4O_9$ samples improve its thermoelectric properties. This improvement is due to a decrease on the electrical resistivity of samples without appreciably modifying the Seebeck coefficient values. The optimal Mn for Co substitution has been determined with respect to the power factor values at 50 and 800 ºC, which is maximum for the 0.03 Mn-doped samples. The raise in PF, compared with the undoped samples, is around 30 % at both temperatures, with values about 0.12 and 0.28 mW K^{-2} m^{-1}, at 50 and 800 ºC, respectively. Moreover, the measured PF values at 800 ºC are around the best ones reported in the literature on high-density Mn-doped materials.

Acknowledgements

The authors wish to thank the Gobierno de Aragón (Research Groups T12 and T87) and the MINECO-FEDER (MAT2013-46505-C3-1-R) for financial support. Authors would also like to acknowledge the use of Servicio General de Apoyo a la Investigación-SAI, Universidad de Zaragoza. The technical contributions of C. Estepa, and C. Gallego are also acknowledged. Sh. Rasekh acknowledges a JAE-PreDoc 2010 grant from CSIC.

References

1. Rowe DM. In: Rowe DM, editor. *Thermoelectrics handbook: macro to nano*. 1st ed. Boca Raton, FL: CRC Press; 2006, 1_3–1_7.

2. G. Mahan, B. Sales and J. Sharp: 'Thermoelectric materials: New approaches to an old problem', *Phys. Today*, 1997, **50**, 42

3. H. Naito, Y. Kohsaka, D. Cooke and H. Arashi: 'Development of a solar receiver for a high-efficiency thermionic/thermoelectric conversion system', *Solar Energy*, 1996, **58**, 191

4. I. Terasaki, Y. Sasago, and K. Uchinokura: 'Large thermoelectric power in $NaCo_2O_4$ single crystals', *Phys. Rev. B*, 1997, **56**, 12685

5. Y. Huang, B. Zhao, J. Fang, R. Ang and Y. Sun: 'Tunning of microstructure and thermoelectric properties of $Ca_3Co_4O_9$ ceramics by high-magnetic-field sintering', *J. Appl. Phys.*, 2011, **110**, 123713

6. A. Sotelo, G. Constantinescu, Sh. Rasekh, M. A. Torres, J. C. Diez and M. A. Madre: 'Improvement of thermoelectric properties of $Ca_3Co_4O_9$ using soft chemistry synthetic methods', *J. Eur. Ceram. Soc.*, 2012, **32**, 2415

7. N. Sun, S. T. Dong, B. B. Zhang, Y. B. Chen, J. Zhou, S. T. Zhang, Z. B. Gu, S. H. Yao and Y. F. Chen: 'Intrinsically modified thermoelectric performance of alkaline-earth isovalently substituted $[Bi_2AE_2O_4][CoO_2]_y$ single crystals', *J. Appl. Phys.*, 2013, **114**, 043705

8. J. C. Diez, E. Guilmeau, M. A. Madre, S. Marinel, S. Lemmonier and A. Sotelo: 'Improvement of $Bi_2Sr_2Co_{1.8}O_x$ thermoelectric properties by laser floating zone texturing', *Solid State Ionics*, 2009, **180**, 827

9. X. G. Luo, Y. C. Jing, H. Chen and X. H. Chen: 'Intergrowth and thermoelectric properties in the Bi-Ca-Co-O system', *J. Crystal Growth*, 2007, **308**, 309

10. A. Sotelo, E. Guilmeau, Sh. Rasekh, M. A. Madre, S. Marinel and J. C. Diez: 'Enhancement of the thermoelectric properties of directionally grown Bi-Ca-Co-O through Pb for Bi substitution', J. Eur. Ceram. Soc. 30, 1815 (2010)

11. R. Ang, Y. P. Sun, X. Luo and W. H. Song: 'A narrow band contribution with Anderson localization in Ag-doped layered cobaltites $Bi_2Ba_3Co_2O_y$', *J. Appl. Phys.*, 2007, **102**, 073721

12. Sh. Rasekh, G. Constantinescu, M. A. Torres, M. A. Madre, J. C. Diez and A. Sotelo: 'Growth rate effect on microstructure and thermoelectric properties of melt grown $Bi_2Ba_2Co_2O_x$ textured ceramics', *Adv. Appl. Ceram.*, 2012, **111**, 490

13. Y. Miyazaki: 'Crystal structure and thermoelectric properties of the misfit-layered cobalt oxides', *Solid State Ionics*, 2004, **172**, 463

14. H. Wang, X. Sun, X. Yan, D. Huo, X. Li, J.-G. Li and X. Ding: 'Fabrication and thermoelectric properties of highly textured $Ca_9Co_{12}O_{28}$ ceramic', *J. Alloys Compds.*, 2014, **582**, 294

15. S. Butt, Y.-C- Liu, J.-L. Lan, K. Shehzad, B. Zhan, Y. Lin and C.-W. Nan: 'High-temperature thermoelectric properties of La and Fe co-doped Ca-Co-O misfit-layered cobaltites consolidated by spark plasma sintering', *J. Alloys Compds.*, 2014, **588**, 277

16. A. Sotelo, E. Guilmeau, M. A. Madre, S. Marinel, S. Lemmonier and J. C. Diez: '$Bi_2Ca_2Co_{1.7}O_x$ thermoelectric ceramics textured by laser floating zone method', *Bol. Soc. Esp. Ceram. V.*, 2008, **47**, 225

17. N. M. Ferreira, Sh. Rasekh, F. M. Costa, M. A. Madre, A. Sotelo, J.C. Diez and M. A. Torres: 'New method to improve the grain alignment and performance of thermoelectric ceramics', *Mater. Lett.*, 2012, **83**, 144

18. J. C. Diez, Sh. Rasekh, M. A. Madre, E. Guilmeau, S. Marinel and A. Sotelo: 'Improved thermoelectrical properties of Bi-M-Co-O (M=Sr, Ca) misfit compounds by laser directional solidification', *J. Electron. Mater.*, 2010, **39**, 1601

19. G. Constantinescu, Sh. Rasekh, M. A. Torres, M. A. Madre, J. C. Diez and A. Sotelo: 'Enhancement of high-temperature thermoelectric performances of $Bi_2Ba_2Co_2O_x$ ceramics', *Scripta Mater.*, 2013, **68**, 75

20. A. Maignan, D. Pelloquin, S. Hébert, Y. Klein and M. Hervieu: 'Thermoelectric power in misfit cobaltites ceramics: Optimization by chemical substitutions', *Bol. Soc. Esp. Ceram. V.*, 2006, **45**, 122

21. G. Constantinescu, Sh. Rasekh, M. A. Torres, J. C. Diez, M. A. Madre and A. Sotelo: 'Effect of Sr substitution for Ca on the $Ca_3Co_4O_9$ thermoelectric properties', *J. Alloys Compds.*, 2013, **577**, 511

22. S. Demirel, M. A. Aksan and S. Altin: 'Low temperature electrical and thermal transport properties of the $Ca_{3-x}Sb_xCo_4O_9$ system', *J. Mater. Sci.: Mater. Electron.*, 2012, **23**, 2251

23. J. C. Diez, M. A. Torres, Sh. Rasekh, G. Constantinescu, M. A. Madre and A. Sotelo: 'Enhancement of $Ca_3Co_4O_9$ thermoelectric properties by Cr for Co substitution', *Ceram. Int.*, 2013, **39**, 6051

24. S. Pinitsoontorn, N. Lerssongkram, N. Keawprak and V. Amornkitbamrung: 'Thermoelectric properties of transition metals-doped $Ca_3Co_{3.8}M_{0.2}O_{9+\delta}$ (M = Co, Cr, Fe, Ni, Cu and Zn)', *J. Mater. Sci.: Mater. Electron.*, 2012, **23**, 1050

25. A. Sotelo, Sh. Rasekh, E. Guilmeau, M. A. Madre, M. A. Torres, S. Marinel and J. C. Diez: 'Improved thermoelectric properties in directionally grown $Bi_2Sr_2Co_{1.8}O_y$ ceramics by Pb for Bi substitution', *Mater. Res. Bull.*, 2011, **46**, 2537

26. J. Liu, H. S. Yang, Y. S. Chai, L. Zhu, H. Qu, C. H. Sun, H. X. Gao, X. D. Chen, K. Q. Ruan and L. Z. Cao: 'Study on the anomalous thermopower and resistivity of (Bi, Pb)–Sr–Co–O: Evidence of a narrow band contribution with Anderson localization', *Phys. Lett. A*, 2006, **356**, 85

27. M. A. Madre, F. M. Costa, N. M. Ferreira, A. Sotelo, M. A. Torres, G. Constantinescu, Sh. Rasekh and J. C. Diez: 'Preparation of high-performance $Ca_3Co_4O_9$ thermoelectric ceramics produced by a new two-step method', *J. Eur. Ceram. Soc.*, 2013, **33**, 1747

28. T. Kajitani, K. Yubuta, X. Y. Huang and Y. Miyazaki: 'Discommensuration of Doped $[Ca_2CoO_3]_pCoO_2$', *J. Electron. Mater.*, 2009, **38**, 1462

29. C. H. Hervoches, H. Okamoto, A. Kjekshus, H. Fjellvag and B. Hauback: 'Crystal structure and magnetic properties of the solid-solution phase $Ca_3Co_{2-v}Mn_vO_6$', *J. Solid State Chem.*, 2009, **182**, 331

30. D. Sedmidubský, V. Jakes, O. Jankovský, J. Leitner, Z. Sofer and J. Hejtmánek: 'Phase equilibria in Ca-Co-O system', *J. Solid State Chem.*, 2012, **194**, 199

31. Y. Wang, Y. Sui, X. Wang, W. Su and X. Liu: 'Enhanced high temperature thermoelectric characteristics of transition metals doped $Ca_3Co_4O_{9+\delta}$ by cold high-pressure fabrication', *J. Appl. Phys.*, 2010, **107**, 033708

32. N. Wu, T. C. Holgate, N. V. Nong, N. Pryds and S. Linderoth: ‘High temperature thermoelectric properties of $Ca_3Co_4O_{9+\delta}$ by auto-combustion synthesis and spark plasma sintering’, *J. Eur. Ceram. Soc.*, 2014, **34**, 925

33. S. B. Chen, H. D. Wang, W. Wan and X. Huang: ‘Homogeneous precipitation synthesis and thermoelectric properties of $Ca_2Co_2O_5$ ceramics‘, *Adv. Appl. Ceram.*, 2013, **112**, 331

34. Sh. Rasekh, M. A. Torres, G. Constantinescu, M. A. Madre, J. C. Diez and A. Sotelo: ‘Effect of Cu by Co substitution on $Ca_3Co_4O_9$ thermoelectric ceramics’, *J. Mater. Sci.: Mater. Electron.*, 2013, **24**, 2309

35. Y. H. Lin, J. Lan, Z. J. Shen, Y. H. Liu, C. W. Nan and J. F. Li: ‘High-temperature electrical transport behaviors in textured $Ca_3Co_4O_9$-based polycrystalline ceramics’, *Appl. Phys. Lett.*, 2009, **94**, 072107

36. S. W. Nam, J. W. Choi, H. K. Hwang and K. Park: ’Improvement in High-Temperature Thermoelectric Properties by Adding Mn for Co in $Ca_3Co_4O_9$’, *J. Nanosci. Nanotech.*, 2010, **10**, 7689

37. Q. Yao, D. L. Wang, L. D. Chen, X. Shi and M. Zhou: ‘Effects of partial substitution of transition metals for cobalt on the high-temperature thermoelectric properties of $Ca_3Co_4O_{9+\delta}$’, *J. Appl. Phys.*, 2005, **97**, 103905

Figure captions:

Figure 1. Powder X-ray diffraction patterns obtained for the $Ca_3Co_{4-x}Mn_xO_y$ samples; x = 0.00 (a); 0.01 (b); 0.03 (c); and 0.05 (d). The diffraction planes indicate the $Ca_3Co_4O_9$ phase and the * the $Ca_3Co_2O_6$ ones. The • symbol identifies the (111) diffraction peak of Si, used as reference.

Figure 2. SEM micrographs performed on representative fractured sections of $Ca_3Co_{4-x}Mn_xO_y$ samples, for x = 0.00 (a); and 0.05 (b).

Figure 3. SEM micrograph performed on a representative surface section, corresponding to the $Ca_3Co_{3.97}Mn_{0.03}O_y$ sample. Major grey contrast corresponds to the $Ca_3Co_{4-x}Mn_xO_y$ phase; #1 indicates the $Ca_3Co_{2-x}Mn_xO_6$ phase.

Figure 4. Temperature dependence of the Seebeck coefficient, as a function of Mn content, in $Ca_3Co_{4-x}Mn_xO_y$ samples, for x = 0.00 (●); 0.01 (■); 0.03 (◆); and 0.05 (▼).

Figure 5. Temperature dependence of the electrical resistivity, as a function of Mn content, in $Ca_3Co_{4-x}Mn_xO_y$ samples, for x = 0.00 (●); 0.01 (■); 0.03 (◆); and 0.05 (▼).

Figure 6. Temperature dependence of the power factor, as a function of Mn content, in $Ca_3Co_{4-x}Mn_xO_y$ samples, for x = 0.00 (●); 0.01 (■); 0.03 (◆); and 0.05 (▼).

Figure 1

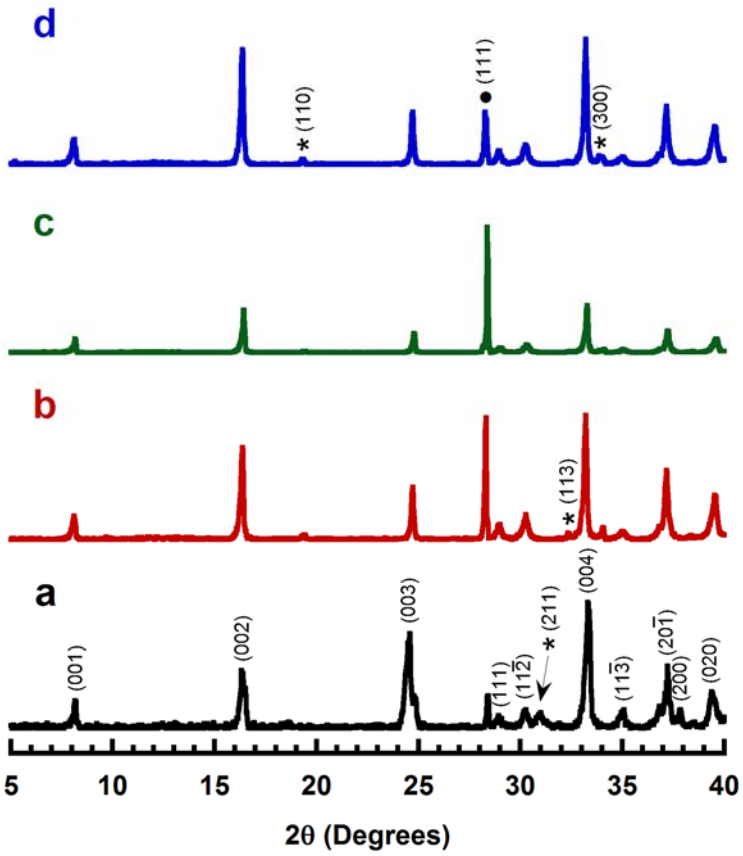
d
c
b
a
(110)
(111)
(300)
(113)
(001)
(002)
(003)
(111)
(112)
(211)
(004)
(113)
(200)
(020)
5
10
15
20
25
30
35
40
2θ (Degrees)

Figure 2

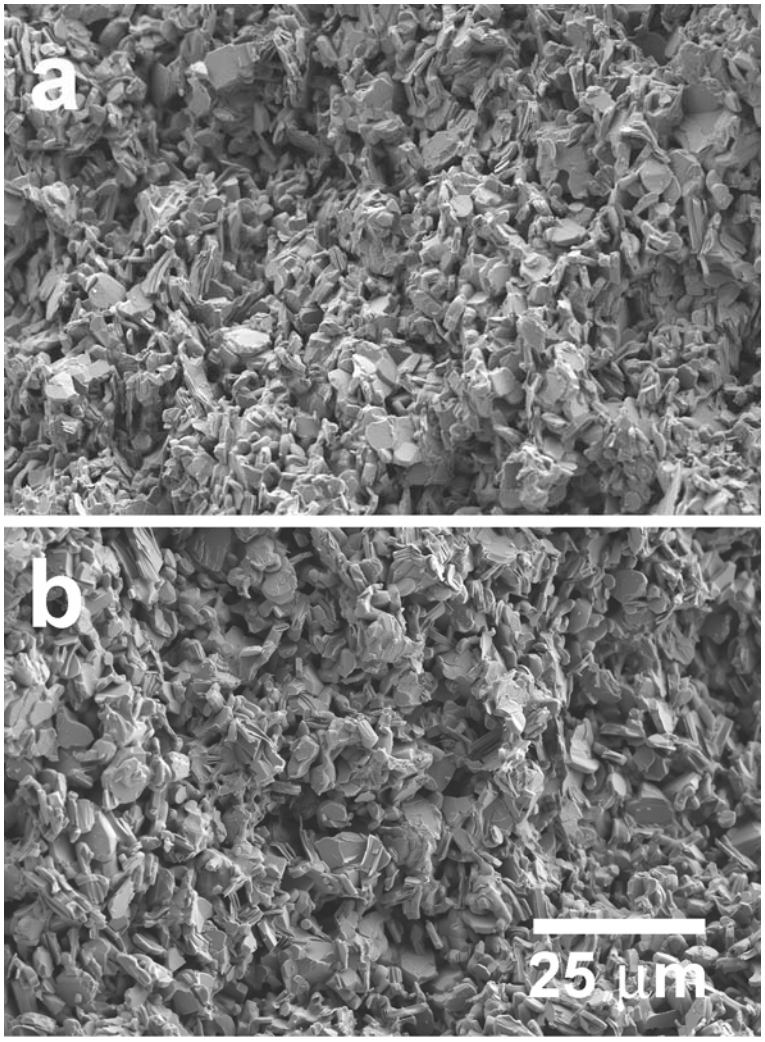

Figure 3

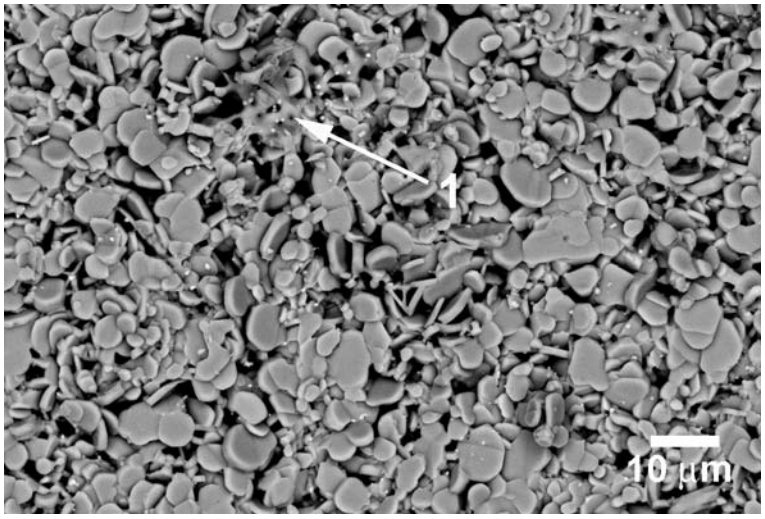

Figure 4

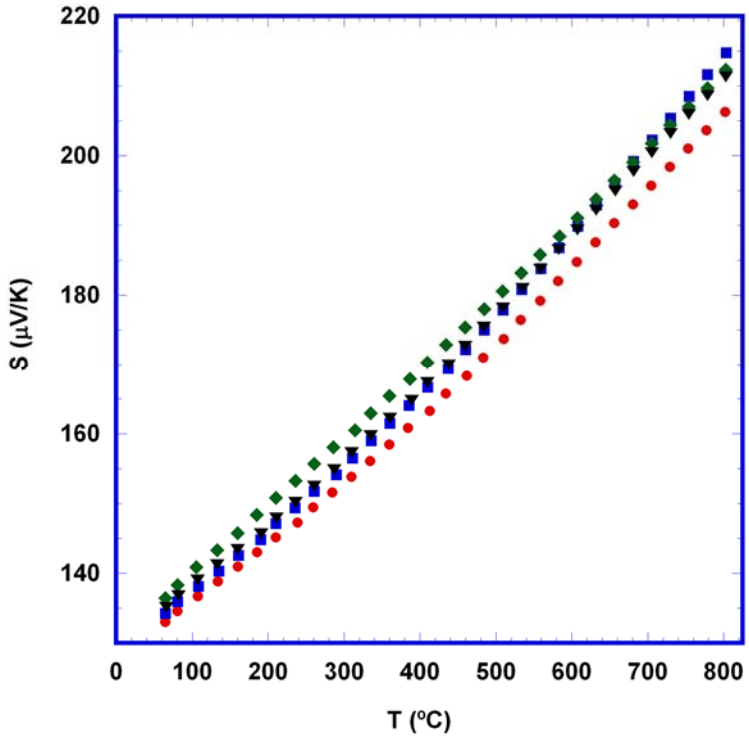

Figure 5

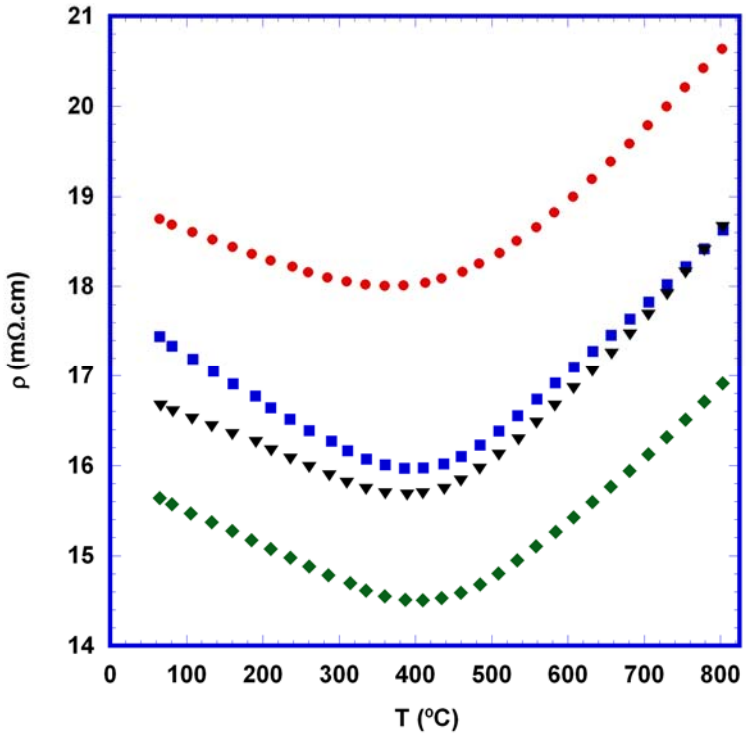

Figure 6